Experiment on antineutrino scattering by electrons at a reactor of the Rovno nuclear power plant

A. I. Derbin, A. V. Chernyĭ, L. A. Popeko, V. N. Muratova, G. A. Shishkina, and S. I. Bakhlanov

B. P. Konstantinov St. Petersbury Institute of Nuclear Physics, 188350 Gatchina, Russia

(Submitted 11 May 1993)
Pis'ma Zh. Eksp. Teor. Fiz. **57**, No. 12, 755–759 (25 June 1993)

A new installation with a 75-kg silicon multidetector in the neutrino laboratory which has been set up at the third unit of the Rovno nuclear power plant is described. The results of the first series of measurements, carried out with the reactor in operation and also shut down, are reported. A new limitation has been obtained on the magnetic moment of the electron antineutrino: $\mu \leqslant 1.5 \times 10^{-10} \mu_B$ (68% C.L.).

1. INTRODUCTION

Work continues at the Rovno nuclear power plant to measure the cross section for neutrino scattering by electrons.[1] The primary reason for the current interest in this scattering is that it would yield the most stringent limitations on the magnetic moment of a neutrino.

2. EXPERIMENTAL APPARATUS

1. Neutrino laboratory. The third unit of the power plant has several rooms which can be used for measurements in a neutrino flux density of $2 \times 10^{13}\ \nu/(\mathrm{cm}^2 \cdot \mathrm{s})$. The primary experiment hall (Fig. 1) is a cast-iron "house" with a mass of 85 metric tons, a wall thickness of 15 cm, and dimensions of $4 \times 4 \times 3.5$ m. The center of the hall is 15 m from the center of the core of the VVR-1000 reactor.

2. Neutrino detector. The silicon multidetector, with a mass of 75 kg, was at the center of the experiment hall. It consisted of 600 Si(Li) detectors ~30 mm in diameter and ~125 mm long. Their characteristics are described in detail in Ref. 2 The multidetector was in a shielded enclosure 360 mm in diameter and 390 mm long, tightly packed, without any internal structural materials. The n^+ lithium contacts of neighboring detectors thus touched each other and were at ground potential. The signals were taken from the central p-type contacts by a lead 20 μm thick in fluoroplastic insulation. They left the first layer of passive shielding through a vacuum connector and went to preamplifiers behind the second layer of passive shielding, 70–100 cm from the detector.

3. Vacuum chamber. The detector, along with the first layer of passive shielding, with a mass of 300 kg, was inside a vacuum chamber 640 mm in diameter and was cooled to liquid-nitrogen temperature. The silicon detectors must be cooled in order to achieve a high energy resolution.

4. Passive shielding. The passive shielding designed to suppress external γ-ray activity consisted of a layer of mercury 80 mm thick and one of copper 150 mm thick.

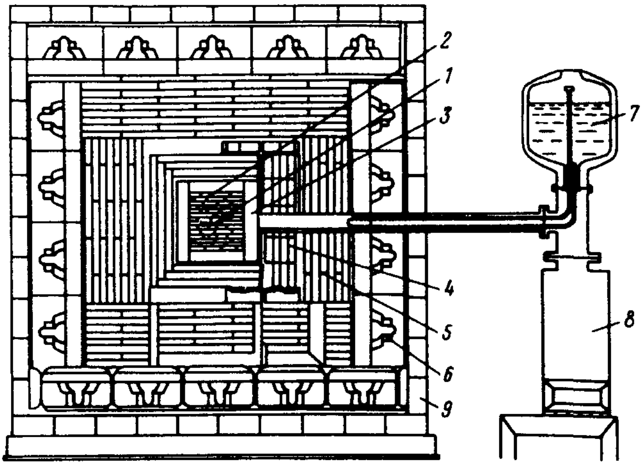

FIG. 1. Experimental apparatus. *1*—HPGe detector at the center of the stack; *2*—600 Si(Li) detectors; *3*—mercury cavity; *4*—copper shielding; *5*—graphite shielding; *6*—active scintillation shielding; *7*—apparatus for cooling the cryostat with liquid nitrogen; *8*—getter-ion pump; *9*—cast-iron "house."

A 500-mm-thick layer of graphite, behind which there was a cadmium absorber, was used as neutron moderator in order to reduce a possible contribution from inverse β decay.

5. *Active shielding.* The active shielding consisted of 120 plastic scintillators with dimensions of $500\times500\times120$ mm in the form of a cube with dimensions of $2.5\times2.5\times2.0$ m. The total load from the active shielding was set at 600 counts/s; with a blanking pulse 150 μs long, the result is a dead time of $\sim10\%$.

3. MEASUREMENT APPARATUS

Each detector had a charge-sensitive preamplifier, an amplifier, a discriminator, linear gates, and an individual bias voltage. The preamplifiers, of discrete design, with dimensions of 5×7 cm, were directly beside the vacuum chamber. The capacitive load was ~150 pF; this figure determined the resolution, ~15 keV. The amplifiers and discriminators were CAMAC-compatible, so a 1M module contained nine channels. The discriminator threshold was automatically set at three times the amplifier noise. The output signals from the discriminators strobed the pulse-height signal and were also fed to a CAMAC bus for storage in the registers of the crate control station, in which a height summation of these signals was carried out. There were 6 such crates, 12 modules in each crate, and 9 channels in each module. Each event in a detector was thus represented in the computer as the status of three registers, with lengths of 9, 12, and 6 bits and by the digitized total height (10 digits).

4. STORAGE OF DATA

In accordance with the status of these registers, 648 spectra were loaded into the memory of the computer (an IBM AT) with 256 channels, corresponding to events in

TABLE I. Count rates of the 37.5-kg detector with the reactor in operation and shut down.

Interval MeV	Operating	Shut down	Open.-Down	Weak scattering	Magnetic scattering
0.2–2.0	15 327±92	14 878±90	449±130	62	178
0.3–2.0	11 193±70	10 908±70	285±98	53	124
0.6–2.0	4962±12	4921± 16	41±20	32	54
1.3–2.0	508.5±4.0	503.3 ±5.6	5.2±6.8	8.9	10

The last two columns give the expected difference in counts according to the standard theory ($\sin^2\theta_W=0.22$) and for the case in which the scattering is due to a magnetic moment of $2\times10^{-10}\,\mu_B$.

an individual detector, and 910 spectra with 32 channels, corresponding to multiple events. The multiplicity was found as the number of nonzero bits in a register. These spectra were saved on disk at 24-h intervals. The number of single events from each detector in the intervals 0.6–2.0 and 1.3–2.0 MeV was put on disk at intervals of 1 h. The energy spectrum of all single events from the multidetector was calculated directly during the data accumulation process; the coefficients of the last calibration were taken into account. These coefficients were determined from the edges of Compton scattering of γ rays from a ^{214}Bi source, which was connected directly to the multidetector with the help of a flexible tube. The "live" time was found with the help of a generator which passed through one of the spectrometer channels. The active shielding was monitored on the basis of the total number of blanking pulses.

5. EXPERIMENTAL RESULTS AND THEIR ANALYSIS

Measurements were taken over 16.7 days with the reactor shut down and over 29.6 days with it operating. The distribution of the count rate as a function of the lower threshold, with the upper threshold at 2.0 MeV, was studied for the series of measurement results obtained. The dispersion was found to exceed that expected statistically up to an energy of 0.6 MeV. This broadening was caused primarily by the active shielding. To obtain a final result we thus removed some detectors, primarily from the inner layers, reducing the detector mass by a factor of nearly 2. For the 37.5-kg detector the average count rate in the interval 0.6–2.0 MeV was 4921 ± 16 day^{-1} with the reactor shut down and 4963 ± 12 day^{-1} with the reactor in operation. The count-rate distribution for the hourly series agrees with a Poisson distribution, both for the individual detectors and for the overall detector. Table I also shows the results for intervals with lower limits of 0.2, 0.3, and 1.3 MeV. The apparent reason why the dispersion found for the first two intervals is much higher than that expected is an instability of the gain (and the steep slope of the background spectrum). The final result for the cross section in the interval 0.6–2.0 MeV is $\sigma=(1.26\pm0.62)\times10^{-44}\,\mathrm{cm}^2$/fission.

6. DISCUSSION OF RESULTS

1. Cross section for neutrino scattering by electrons. The result found corresponds

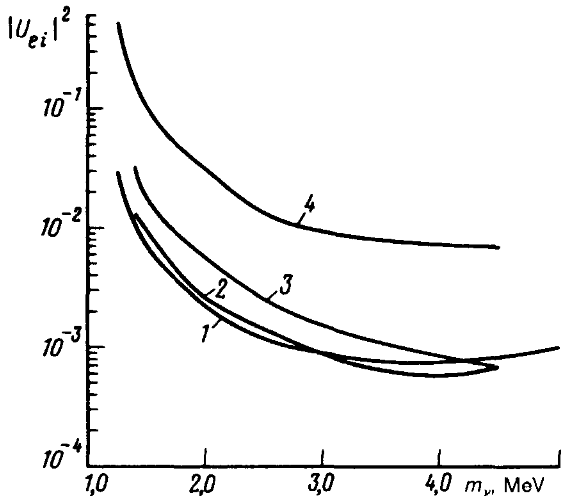

FIG. 2. Limitation on a possible admixture of a massive neutrino in the β decay of fission fragments of the nuclear fuel. 2, 3, 4—from the experiments of Refs. 11, 10, and 9, respectively.

to $\sigma=(1.28\pm0.63)\sigma_{W-S}$, where σ_{W-S} is the cross section expected in the standard theory on the basis of calculations with the reactor-neutrino spectrum from Ref. 3 and $\sin^2\theta_W=0.22$.

2. Limitation on the magnetic moment of the neutrino. In connection with a possible explanation of the deficiency of solar neutrinos,[4] there is interest in a limitation on a possible magnetic moment of a neutrino. Since the weak and magnetic scattering processes do not interfere, we can take the sum of the error and the deviation from the expected value as a limitation on this magnetic moment. In this case, using the result cited above for the cross section in the interval 0.6–2.0 MeV, we find $\mu\leqslant 1.5\times10^{-10}\ \mu_B$ (68% C.L.) or $\mu\leqslant 1.9\times10^{-10}\ \mu_B$ (95% C.L.). The best existing limitation on the neutrino magnetic moment was found from the experiments of Ref. 5: $\mu\leqslant(2-4)\times10^{-10}\ \mu_B$.[6,7] A limit $\mu\leqslant2.4\times10^{-10}\ \mu_B$ was recently found[8] from measurements of the cross section for (ν, e) scattering.

3. Limitation on possible neutrino decay. If neutrinos have masses and are mixed, it might be possible to observe decays of the more massive neutrino. As the most likely detectable decay modes we consider the radiative decay $(\nu\to\nu+\gamma)$ and the decay $\nu\to\nu+e^+e^-$.[9] In the former case, under the assumption that a Dirac neutrino strongly bound with an electron decays $(U_{ie}\approx1)$, we find a limitation on the lifetime: $\tau_{c.m.}/m_\nu\geqslant200$ s/eV. This is nine times as large as the limitation found in the experiment of Ref. 10. Decay into an e^+e^- pair requires a neutrino mass greater than $2m_e$, and the decay probability would depend on both the neutrino mass and the mixing angle U_{ie} $(\ll1)$. Accordingly, the limitation on the probability for such a decay, plotted as U_{ie} vs m_ν, would look like the curve in Fig. 2. Shown for comparison here are curves from other experiments.

7. CONCLUSION

Preparations are currently under way for a new series of measurements with a detector of modified construction. These experiments are aimed at energies of about 100 keV, where the cross section expected for magnetic scattering is an order of magnitude greater than near 0.6 MeV.

[1] A. V. Derbin, L. A. Popeko, A. V. Chernyĭ, and G. A. Shishkina, JETP Lett. **43**, 206 (1986).
[2] S. Bakhlanov, A. V. Derbin, V. Muratova *et al.*, Preprint LIYaF-864, Leningrad Institute of Nuclear Physics, 1983.
[3] K. Schreckenbach *et al.*, Phys. Lett. B **160**, 325 (1985); A. A. Hahn, K. Schreckenbach, and W. Gelletly, Phys. Lett. B **218**, 365 (1989).
[4] M. B. Voloshin, M. I. Vysotskiĭ, and L. B. Okun', Zh. Eksp. Teor. Fiz. **91**, 754 (1986) [Sov. Phys. JETP **64**, 446 (1986)].
[5] R. Reines, H. Curr, and H. Sobel, Phys. Rev. Lett. **37**, 315 (1976).
[6] A. V. Kyuldiev, Nucl. Phys. B **243**, 387 (1984).
[7] P. Vogel and J. Engel, Phys. Rev. D **39**, 3378 (1989).
[8] I. I. Gurevich *et al.*, *Proc. of the LEWI-90* (Dubna, 1991), p. 173.
[9] P. Vogel, Phys. Rev. D **30**, 1505 (1984).
[10] L. Oberaver, F. V. Feilitzsch, and R. L. Mossbauer, Phys. Lett. B **198**, 113 (1987).
[11] V. I. Kopeĭkin, L. A. Mika'elyan, and S. A. Fayans, JETP Lett. **51**, 86 (1990).

Translated by D. Parsons